Published in final edited form as:
Bioconjug Chem. 2013 July 17; 24(7): 1191–1200. doi:10.1021/bc400084u.

Development of a new thiol site-specific prosthetic group and its conjugation with [cys^{40}]-exendin-4 for in vivo targeting of insulinomas

Xuyi Yue[1,2], **Dale O. Kiesewetter**[1], **Jinxia Guo**[1,2], **Zhongchan Sun**[1], **Xiaoxiang Zhang**[1], **Lei Zhu**[1,2], **Gang Niu**[1], **Ying Ma**[1], **Lixin Lang**[1], and **Xiaoyuan Chen**[1,*]

[1]National Institute of Biomedical Imaging and Bioengineering (NIBIB), National Institutes of Health (NIH), 31 Center Drive, Bethesda, Maryland 20892, United States

[2]Center for Molecular Imaging and Translational Medicine, School of Public Health, Xiamen University, Xiamen, 361005, China

Abstract

A new tracer, *N*-5-[^{18}F]fluoropentylmaleimide ([^{18}F]FPenM), for site-specific labeling of free thiol group in proteins and peptides was developed. The tracer was synthesized in three steps (^{18}F displacement of the aliphatic tosylate, di-Boc removal by TFA to expose free amine and incorporation of the free amine into a maleimide). The radiosynthesis was completed in 110 min with 11–17% radiochemical yield (uncorrected), and specific activity of 20–49 GBq/μmol. [^{18}F]FPenM showed comparable labeling efficiency with *N*-[2-(4-[^{18}F]fluorobenzamido)ethyl]maleimide ([^{18}F]FBEM). Its application was demonstrated by conjugation with glucagon-like peptide type 1 (GLP-1) analogue [cys^{40}]-exendin-4. The cell uptake, binding affinity, imaging properties, biodistribution and metabolic stability of the radiolabeled [^{18}F]FPenM-[cys^{40}]-exendin-4 were studied using INS-1 tumor cells and INS-1 xenograft model. Positron emission tomography (PET) results showed that the new thiol-specific tracer, [^{18}F]FPenM-[cys^{40}]-exendin-4, had high tumor uptake (20.32 ± 4.36 %ID/g at 60 min post-injection) and rapid liver and kidney clearance, which was comparable to the imaging results with [^{18}F]FBEM-[cys^{40}]-exendin-4 reported by our group.

Introduction

Receptor targeting with radiolabeled peptides is an important and successful method for the diagnosis and treatment of neuroendocrine tumors[1]. The most prominent clinically applied peptides for *in vivo* imaging of human tumors are the somatostatin analogues[2]. The overexpression of many peptide receptors in cancers, compared to their relatively low density in normal organs, provides the rationale for *in vivo* molecular imaging and targeted radionuclide therapy. Among the available positron emitters for peptide labeling, fluorine-18 (^{18}F) is most used due to its nuclear decay properties and chemical properties. The nuclide decays with a relatively low positron emission energy of 0.64 MeV, which provides a short tissue range (0.46 mm) and thus the potential for high image resolution. Its half-life (109.8

*Corresponding Author: Shawn.Chen@nih.gov.

ASSOCIATED CONTENT

Supporting Information. Serum stability of [^{18}F]FPenM-[cys^{40}]-exendin-4. Metabolite analysis of [^{18}F]FPenM-[cys^{40}]-exendin-4 in the tumor, kidneys and urine. This material is available free of charge via the Internet at http://pubs.acs.org.

Notes

The authors declare no competing financial interest.

min) is long enough to allow complex, multistep radiosynthesis and allows image acquisitions for two or more hours post-injection. Labeling of organic molecules with ^{18}F is amply described in the literature[3–6].

Only a few examples for direct labeling of peptides or other macromolecules have been reported[7–11], due to the harsh reaction conditions typically employed for ^{18}F incorporation. To circumvent this drawback, a prosthetic group carrying the radioisotope is prepared and subsequently conjugated to a reactive functionality of macromolecule under mild conditions. *N*-succinimidyl-4-[^{18}F]fluorobenzoate ([^{18}F]SFB) is the most widely used ^{18}F-prosthetic group for labeling peptides and proteins by conjugation of amine groups under mildly basic conditions (pH 8) and temperatures less than 40 °C[12–17]. Sometimes peptide labeling with [^{18}F]SFB gives poor yield due to the steric hindrance of amino groups or unanticipated chemoselectivity and regioselectivity due to abundance of free amino groups in protein[18, 19]. Furthermore, a stoichiometric excess of valuable protein or peptide is often required to achieve sufficient radiochemical yields.

Alternative ^{18}F-prosthetic groups for peptide labeling are maleimide-containing compounds that provide site-specific labeling of free thiol groups. Peptides and proteins can be engineered to incorporate or expose one cysteine residue to provide a site for specific labeling[20, 21]. There are several reports using maleimides as prosthetic groups for ^{18}F PET study (Figure 1). The recently used ^{18}F-prosthetic groups for thiol functions include [^{18}F]FPPD and [^{18}F]DDPFB developed by Shiue *et al.*[22]; aminooxy-aldehyde condensation series such as [^{18}F]FBABM[23], [^{18}F]FBAM[24], and [^{18}F]FBOM[25], which contained an aldehyde-reactive aminooxy group and a thiol-reactive maleimide group *via* readily available 4-[^{18}F]fluorobenzaldehyde. [^{18}F]FDG-MHO, another aminooxy-aldehyde condensation agent for thiol-specific labeling based on [^{18}F]FDG was developed by Wuest *et al.*[26]. Dollé's group reported the preparation of a heteroaromatic [^{18}F]maleimide, 1-[3-(2-[^{18}F]fluoropyridine-3-yloxy)propyl]pyrrole-2,5-dione ([^{18}F]FPyME) in three steps with 17–20% uncorrected radiochemical yield[27]. *N*-[2-(4-[^{18}F]fluorobenzamido)ethyl]maleimide ([^{18}F]FBEM) is among the most often used prosthetic groups for site-specific radiolabeling of the free sulfhydryl groups of peptides and proteins. Two groups reported its synthetic methodology, either from previously reported [^{18}F]SFB precursor[28] or through more efficient direct condensation of 4-[^{18}F]fluorobenzoic acid with *N*-(2-aminoethyl)maleimide[29] with high specific activity. The other [^{18}F]FBEM analogue, 4-[^{18}F]fluorobenzylamidopropionyl maleimide ([^{18}F]FBAPM) was synthesized through four radiolabeling steps with 55% decay corrected yield in 70 min and specific activity of 50–70 GBq/μmol. The route features highly efficient reduction of nitrile group using borohydride/transition metal catalyst method[30].

Recently, several investigators reported novel bifunctional prosthetic groups containing a maleimide group and a moiety for incorporation of [^{18}F]fluoride in a single step. Inkster *et al.* reported sulfonyl fluoride-based prosthetic compounds as potential ^{18}F labeling agents under aqueous conditions. One of the prosthetic groups, 4-*N*-maleimidobenzenesulfonyl [^{18}F]fluoride ([^{18}F]FBSM) was prepared in moderate yield, but the solvent and base selection during the preparation have a profound influence on the yield, and the exemplified ^{18}F-peptide showed evidence of proteolytic defluorination and modification during incubation with mouse serum[31]. McBride *et al.*, in an extension of their highly successful chelation of [^{18}F]aluminum fluoride, developed [^{18}F]AlF-NODA-MPAEM. This prosthetic group was conjugated to antibody Fab' fragment at room temperature in high yield without much loss of immunoreactivity. The method is useful for heat labile compounds[32] (Figure 1).

With the exceptions of [^{18}F]FDG-MHO, [^{18}F]AlF-NODA-MPAEM and [^{18}F]FBSM, the above described radiofluorinations have been limited to nucleophilic aromatic substitutions. Activated aromatic rings bearing both a good leaving group and a strong electron-withdrawing component, especially located *para* to the leaving group are required during radiolabeling. However, heteroaromatic and aliphatic nucleophilic substitutions only require a good leaving group and the reactions are usually performed with dried no-carrier-added [^{18}F]fluoride under basic conditions[27, 33]. Here we developed a new aliphatic maleimide-based prosthetic group based on aliphaticnucleophilic substitution. It was used for labeling GLP-1 receptor targeted peptide [cys^{40}]-exendin-4 as an example (Figure 2).

Our group developed two new exendin-4 analogues by incorporation of a cysteine residue to either the C- or N-terminus of exendin-4, then site-specifically labeled with maleimide-containing prosthetic group [^{18}F]FBEM[34] or [^{18}F]AlF-NOTA-MAL[35]. Results showed that both [^{18}F]FBEM-[cys^{40}]-exendin-4 and [^{18}F]AlF-NOTA-MAL-[cys^{40}]-exendin-4 have high tumor uptake but exhibit significantly different kidney uptake and clearance. In order to develop a more rapid radiochemical synthesis of a maleimide-based prosthetic group and to better understand the effect of the prosthetic group on the imaging profile of peptides, we describe here a new thiol-specific prosthetic agent, *N*-5-[^{18}F]fluoropentylmaleimide ([^{18}F]FPenM) based on aliphatic nucleophilic substitution and its conjugation with [cys^{40}]-exendin-4. This new bifunctional agent has the lowest molecular weight among the maleimide-based tracers reported and, thus, would be expected to have a minimal effect on binding affinity compared to the parent exendin-4. The cell uptake, biodistribution, and imaging properties of [^{18}F]FPenM-[cys^{40}]-exendin-4 are described.

Experimental Section

Reagents and instrumentation

Unless otherwise stated, all chemicals were obtained from commercial sources and used without further purification. Analytical thin layer chromatography (TLC) was performed on Merck precoated silica gel 60 F254 plates with visualization by ultraviolet (UV) irradiation at λ = 254 nm or staining with $KMnO_4$. Purifications were performed by silica gel chromatography. The water used in the experiments with [cys^{40}]-exendin 4 (FW 4289.69) was deionized from Milli-Q Integral Water Purification System. [cys^{40}]-exendin-4 was prepared by solid-phase peptide synthesis (CS Bio, Menlo Park, CA, USA). The [cys^{40}]-exendin-4 sequence is His-Gly-Glu-Gly-Thr-Phe-Thr-Ser-Asp-Leu-Ser-Lys-Gly-Met-Glu-Glu-Glu-Ala-Val-Arg-Leu-Phe-Ile-Glu-Trp-Leu-Lys-Asn-Gly-Gly-Pro-Ser-Ser-Gly-Ala-Pro-Pro-Pro-Ser-Cys-NH_2.

Mass Spectrometry

LC/MS analysis was conducted on a Waters LC-MS system (Waters, Milford, MA) that included an Acquity UPLC unit coupled to the Waters Q-Tof Premier high resolution mass spectrometer. An Acquity BEH Shield RP18 column (150 × 2.1 mm) was employed for chromatography. Elution was achieved with isocratic 2 mM ammonium formate, 0.1% formic acid, and 5% CH_3CN at 0.35 mL/min, The entire column elute was introduced into the Q-Tof mass spectrometer. Ion detection was achieved in ESI mode using a source capillary voltage of 3.5 kV, source temperature of 110 °C, desolvation temperature of 200 °C, cone gas flow of 50 L/Hr (N_2), and desolvation gas flow of 700 L/Hr (N_2).

Chemistry

Compounds **1**[36], **4a**[37], **4b**[38], **4c**[39], **5a**[40] (Scheme 1) are known compounds and were prepared according to literature procedures. Their physical and spectroscopic data are in agreement with those previously reported.

1-(2-fluoroethyl)-1H-pyrrole-2,5-dione, 2

Fluoroethylamine hydrochloride (110 mg, 2.2 mmol) was dissolved in a saturated aqueous solution of sodium bicarbonate (4 mL). The solution was cooled to 0 °C and stirred for 10 min before adding *N*-(methoxycarbonyl)maleimide **1** (310 mg, 2 mmol). The resulting solution was stirred at 0 °C for 10 min and at room temperature for an additional 20 min and the reaction was monitored by TLC. The mixture was directly subjected to silica gel flash chromatography using hexane/EtOAc (3/1) as the eluent to afford compound **2** (150 mg, 1.05 mmol, 53% yield) as a colorless solid. ^{1}H NMR (300 MHz, $CDCl_3$) δ 6.72 (s, 2H), 4.58 (t, J = 5.1 Hz, 1H), 4.42 (t, J = 4.8 Hz, 1H), 3.84 (t, J = 5.1 Hz, 1H), 3.76 (t, J = 5.1 Hz, 1H); ^{13}C NMR (75.5 MHz, $CDCl_3$) δ 170.5, 134.4, 80.5 (d, J = 171.4 Hz), 38.2 (d, J = 21.9 Hz); ^{19}F NMR (282 MHz, $CDCl_3$) δ −224.7 ∼ −225.2 (m); MS (APCI) 144.0 $[M + H]^+$; HRMS (APCI): Calcd for $C_6H_7NO_2F$, 144.0461 $[M + H]^+$, found 144.0457.

Typical procedure for the synthesis of compounds 2-[bis(tert-butoxycarbonyl)amino]ethoxy(4-methylphenyl)-dioxo-λ^6-sulfane 5a, 3-[bis(tert-butoxycarbonyl)amino]propoxy(4-methylphenyl)-dioxo-λ^6-sulfane 5b, and 5-[bis(tert-butoxycarbonyl)amino]pentoxy(4-methylphenyl)-dioxo-λ^6-sulfane 5c

Commercial di-*tert*-butyl iminodicarboxylate (1 eq.) was dissolved in ethanol and treated with 1.1 equivalents of 40% aqueous *n*-$Bu_4N^+OH^-$ at room temperature for 1 h. The solvents were removed and the residue dried by repeated evaporation with acetonitrile. To the solution of the resulting salt in acetonitrile was added the bis-tosylate of ethylene glycol (1.1 eq.). The resulting solution was stirred at room temperature and monitored by TLC until the starting material was completely consumed. The reaction solution was diluted with water and extracted with CH_2Cl_2. The organic layer was dried and evaporated. The residue was subjected to flash chromatography using hexane/EtOAc (4/1) as the eluent to give the title compound **5**.

Compound 5a—Colorless solid, 2.44 g, yield 64%. ^{1}H NMR (300 MHz, $CDCl_3$) δ 7.72 (d, J = 6.6 Hz, 2H), 7.30 (d, J = 8.1 Hz, 2H), 4.07 (t, J = 5.7 Hz, 2H), 3.83 (t, J = 5.7 Hz, 2H), 2.38 (s, 3H), 1.42 (s, 18H).

Compound 5b—Colorless solid, 1.32 g, yield 62%. ^{1}H NMR (300 MHz, CD_3OD) δ 7.81 (d, J = 8.4 Hz, 2H), 7.47 (d, J = 8.1 Hz, 2H), 4.08 (t, J = 6.3 Hz, 2H), 3.64 (t, J = 6.6 Hz, 2H), 2.47 (s, 3H), 1.91 (t, J = 7.2 Hz, 2H), 1.53 (s, 18H); ^{13}C NMR (75.5 MHz, $CDCl_3$) δ 153.9, 146.6, 134.6, 131.3, 129.2, 84.1, 69.9, 29.9, 28.4, 21.7; MS (APCI) 447.2 $[M + NH_4]^+$; HRMS (APCI): Calcd for $C_{20}H_{35}N_2O_7S$, 447.2165 $[M + NH_4]^+$, found 447.2166.

Compound 5c—Liquid, 0.41g, yield 45%. ^{1}H NMR (300 MHz, CD_3OD) δ 7.92 – 7.89 (m, 2H), 7.56 (d, J = 7.8 Hz, 2H), 4.18 – 4.14 (t, J = 6.3 Hz, 2H), 3.67 – 3.61 (m, 2H), 2.57 (s, 3H), 1.83 – 1.72 (m, 2H), 1.70 – 1.65 (m, 2H), 1.64 (s, 18H), 1.57 – 1.41 (m, 2H); ^{13}C NMR (75.5 MHz, $CDCl_3$) δ 154.0, 146.3, 134.6, 131.2, 128.9, 83.5, 71.8, 47.0, 29.5, 29.4, 28.5, 23.7, 21.8; MS (APCI) 475.2 $[M + NH_4]^+$; HRMS (APCI): Calcd for $C_{22}H_{39}N_2O_7S$, 475.2478 $[M + NH_4]^+$, found 475.2478.

Typical procedure for the synthesis of 1-(3-fluoropropyl)-1H-pyrrole-2,5-dione 8b and 1-(5-fluoropentyl)-1H-pyrrole-2,5-dione 8c

To a test tube with a stirring bar was added K_{222} (1 eq.) in acetonitrile (1 mL), and potassium fluoride (2 eq.). The solvents were evaporated under a stream of argon while being heated in a 100 °C oil bath. Three portions of acetonitrile (1 mL) were added successively and each evaporated in turn. Then tosylate substrate **5b** (or **5c**) (1 eq.) in acetonitrile (1 mL) was added. The reaction solution was heated at 100 °C for 20 min. The

solvent was removed under a stream of argon. The residue was treated with TFA (1 mL) at room temperature for 10 min. After evaporation of TFA with argon flow, the reaction was placed in 0 °C ice water, saturated sodium bicarbonate (4 mL) and *N*-(methoxycarbonyl)maleimide (2 eq.) was added successively. The solution was stirred at 0 °C for 20 min and then at room temperature for 10 min, then subjected to silica gel chromatography directly using hexane/EtOAc (4/1) as the eluent to afford compound **8b** (or **8c**).

Compound 8b—Colorless solid, 28% yield for three steps, ^{1}H NMR (300 MHz, $CDCl_3$) δ 6.73 (s, 2H), 4.56 (t, *J* = 5.7 Hz, 1H), 4.41 (t, *J* = 5.7 Hz, 1H), 3.70 (t, *J* = 6.9 Hz, 2H), 2.08 – 2.04 (m, 1H), 1.99 – 1.95 (m, 1H); ^{13}C NMR (75.5 MHz, $CDCl_3$) δ 170.9, 134.4, 81.8 (d, *J* = 166.1 Hz), 34.8 (d, *J* = 21.0 Hz), 29.6 (d, *J* = 78.0 Hz); ^{19}F NMR (282 MHz, $CDCl_3$) δ −220.9 ∼ −221.4 (m); MS (APCI) 158.1 $[M + H]^+$; HRMS (APCI): Calcd for $C_7H_9NO_2F$, 158.0617 $[M + H]^+$, found 158.0612.

Compound 8c—Liquid, 62% yield for three steps, ^{1}H NMR (300 MHz, $CDCl_3$) δ 6.71 (s, 2H), 4.53 (t, *J* = 6.0 Hz, 1H), 4.37 (t, *J* = 6.0 Hz, 1H), 3.56 (t, *J* = 7.2 Hz, 2H), 1.81 – 1.60 (m, 4H), 1.48 – 1.28 (m, 2H); ^{13}C NMR (75.5 MHz, $CDCl_3$) δ 171.0, 134.3, 84.0 (d, *J* = 164.6 Hz), 37.8, 30.1 (d, *J* = 78.0 Hz), 28.4, 22.7 (d, *J* = 21.0 Hz); ^{19}F NMR (282 MHz, $CDCl_3$) δ −218.4 ∼ −218.9 (m); MS (APCI) 186.1 $[M + H]^+$; HRMS (APCI): Calcd for $C_9H_{13}NO_2F$, 186.0930 $[M + H]^+$, found 186.0927.

General procedure for the synthesis of nonradioactive fluoroalkylmaleimido-[cys^{40}]-exendin-4

[cys^{40}]-exendin-4 was dissolved in degassed phosphate-buffered saline (PBS), N-2-fluoroethylmaleimde or N-5-fluoropentylmaleimide in EtOH was added in one portion and incubated for 1 h, then the mixture was subjected to semi-preparative HPLC chromatography to give N-2-fluoroethylmaleimido-[cys^{40}]-exendin-4 and N-5-fluoropentylmaleimido-[cys^{40}]-exendin-4, respectively. For semi-preparative HPLC, a Vydac C_{18} protein column (9.4 × 250 mm) and a gradient elution profile were used with 0.1% trifluoroacetic acid (TFA) in water (solvent A) and 0.1% TFA in CH_3CN (solvent B). The elution profile was isocratic at 25% solvent B for 5 min, then a gradient to 55% solvent B over 20 min, and finally to 90% B over the next 5 min. The major peak at about 17 min was collected and lyophilized. For analytical HPLC, a Vydac C_{18} protein column (4.6 × 250 mm) was used with a gradient elution profile using water (solvent A), CH_3CN (solvent B), 1 mM $EDTANa_2$, and 1% TFA in water (solvent C). The gradient used was 65% water, 25% acetonitrile, 10% solvent C for 5 min, then a linear gradient to 35% water, 55% acetonitrile, 10% solvent C by 25 min, and a linear gradient to 90% acetonitrile, 10% solvent C at 30 min.

Typical procedure for the synthesis of compounds [^{18}F]8a, [^{18}F]8b and [^{18}F]8c

To a test tube was added K_{222} (4.5 mg, 12 μmol in 100 μL acetonitrile), K_2CO_3 (60 μL of 0.1 M in water, 6 μmol), and [^{18}F]fluoride (59 – 77 mCi). The solvents were evaporated under a stream of argon while being heated in a 100 °C heating block. Three portions of acetonitrile (200 μL) were added successively and each evaporated in turn, the drying procedure took about 10 min. Then tosylate **5** (2.5 – 3.0 mg, 6.0 μmol) in acetonitrile (200 μL) was added. The reaction solution was heated at 100 °C for 10 min. The reaction solution was cooled to room temperature and diluted with CH_2Cl_2 (200 μL); the mixture was loaded onto a short plug of silica gel and eluted with another portion of CH_2Cl_2 (400 μL) into a 13 × 100 mm test tube. The isolated yield for this radiolabeling step was calculated by dividing the amount of activity in the eluent by the total initial activity used. The eluate was evaporated to dryness under a stream of argon at room temperature. Trifluoroacetic acid

(TFA, 200 μL) was added to the residue and allowed to stand for 5 min. The TFA was evaporated with a stream of argon. The reaction tube was then cooled in an ice bath and the following reagents were added in sequence: saturated $NaHCO_3$ (450 μL); and *N*-(methoxycarbonyl)maleimide (9.3 mg, 60 μmol) in THF (150 μL). Five min later, the solution was diluted with 0.1% TFA in H_2O (0.3 mL), and subjected to semi-preparative HPLC directly (Phenomenex Luna 5 μm C_{18} column, 250 × 10 mm, flow rate 4.0 mL/min, solvent A, 0.1% TFA in water, solvent B, 0.1% TFA in acetonitrile, using isocratic with 30% solvent B, UV detection at 210 nm and on-line radioactivity detection, product t_R = 26.1 min). The collected fraction (typically 19 – 28% uncorrected yield) was diluted with 10 mL water and the product was trapped on a Sep-Pak C_{18} plus cartridge (360 mg sorbent per cartridge). The cartridge was washed with H_2O (3 mL) and hexane (2 mL), and the product was eluted with 10% EtOH in CH_2Cl_2 (1.5 mL). The solvent was removed under argon flow. The three-step radiolabeling was completed in an average time of 110 min with 11–17% uncorrected yield.

For quality control, the concentrated sample was analyzed by analytical HPLC (Phenomenex Luna 3 μm C_{18} column, 150 × 4.6 mm, flow rate 1.0 mL/min, solvent A, 0.1% TFA in water, solvent B, 0.1% TFA in acetonitrile), using isocratic elution with 35% solvent B; product eluted at 8.1 min. Specific activity was estimated at 210 nm of wavelength by comparison with a standard curve.

Radiochemical synthesis of [^{18}F]FPenM-[cys^{40}]-exendin-4

To the above [^{18}F]FPenM (8–11 mCi) was added ethanol (10 μL) and the tube was vortexed. [cys^{40}]-exendin-4 (100–200 μg) in 100 μL 0.1% sodium ascorbate in degassed PBS was added, and the solution was vortexed followed by incubation for 30 min at room temperature. Aqueous TFA (0.1% TFA, 100 μL) was added and the solution was injected onto a semi-preparative HPLC system (as described above for nonradioactive fluoroalkylmaleimido-[cys^{40}]-exendin-4 with the exception that the first gradient went only to 45% B over 30 min). The elution time of the radioactive product was about 29.3 min. The fraction containing [^{18}F]FPenM-[cys^{40}]-exendin-4 was diluted to 20 mL with water and the solution passed through a C_{18} BondElut cartridge (100 mg). The product that remained on the cartridge was eluted with 1 mL of 10 mM HCl in ethanol. The ethanol was concentrated on a rotary evaporator to about 100 – 200 μL. A portion of this remaining volume was used for determination of radiochemical purity. The remaining volume was diluted in PBS for *in vitro* and *in vivo* studies. For quality control, the same analytical HPLC condition as preparation of nonradioactive fluoroalkylmaleimido-[cys^{40}]-exendin-4 was used. HPLC-MS 1119.4 $[M + 4H]^{4+}$; deconvolves to 4474.0. Calculated exact mass: $C_{196}H_{299}FN_{52}O_{63}S_2$ (4474.128).

Mouse serum stability study

[^{18}F]FPenM-[cys^{40}]-exendin-4 (50 μCi) was mixed with 200 μL freshly harvested mouse serum and a 50 μL aliquot was removed at 0 min. The remainder was incubated at 37 °C and additional aliquots of 50 μL were removed at 30 and 150 min. The aliquots were mixed with an equal volume of CH_3CN and centrifuged. A portion of the supernatant was subjected to radioHPLC analysis using an on-line radioactivity detector.

Cell culture

INS-1 cell line was cultured in RPMI-1640 medium (GIBCO) containing 10% (v/v) fetal bovine serum (GIBCO) supplemented with penicillin (100 μg/mL), streptomycin (100 μg/mL), non-essential amino acids (100 μM) and sodium pyruvate (1 mM) at 37 °C with 5% CO_2.

Animal model

All animal studies were conducted in accordance with the principles and procedures outlined in the Guide for the Care and Use of Laboratory Animals and were approved by the Institutional Animal Care and Use Committee of Clinical Center, NIH. The INS-1 xenograft tumor models were developed in 5 to 6-week old female athymic nude mice (Harlan Laboratories) by injection of 5×10^6 cells in the left or right shoulders. Tumor growth was monitored using caliper measurements of perpendicular axes of the tumor. The tumor volume was estimated by the formula: tumor volume = $a \times (b^2)/2$, where a and b were the tumor length and width, respectively, in millimeters. The mice underwent small-animal PET studies when the tumor volume reached 100–300 mm^3 (3–4 weeks after inoculation).

Receptor binding assay

The GLP-1 receptor binding assay was performed to determine binding affinities of FEtM-[cys^{40}]-exendin-4, FPenM-[cys^{40}]-exendin-4, FBEM-[cys^{40}]-exendin-4, and exendin-4. GLP-1 analogs were dissolved in DMSO and diluted by cell binding buffer (1 mM $CaCl_2$, 5 mM $MgCl_2$, 0.5% BSA in RPMI medium) to the desired concentrations immediately before usage. At 80% confluence, the cultured cells were scraped off and suspended in binding buffer at a final concentration of 2×10^6 cells/mL. The cells were aliquoted into a 96 well plate (1×10^5 INS-1 cells/well) and incubated with ^{125}I-GLP-1(7–36) (0.02 μCi/well, PerkinElmer, Inc) in binding buffer in the presence of different concentrations of GLP-1 analogs at room temperature for 2 h. The final volume per well is 200 μL. After incubation, the plate was washed three times with PBS containing 0.1% BSA, and the radioactivity was measured by γ-counting. The IC_{50} values were calculated by nonlinear regression analysis using the GraphPad Prism computer-fitting program (GraphPad Software, Inc., San Diego, CA). Each data point is a result of the average of duplicate wells.

Cell uptake and efflux studies

For cell uptake, INS-1 cells were seeded into 24-well plates at a density of 1×10^5 cells per well and incubated with 37 kBq (1 μCi) per well of [^{18}F]FPenM-[cys^{40}]-exendin-4 in 500 μL of serum free cell culture medium at 37 °C for 15, 30, 60, and 120 min. The cells were then washed three times with chilled PBS and lysed with 200 μL 0.1 M NaOH. For efflux studies, about 37 kBq (1 μCi) per well of [^{18}F]FPenM-[cys^{40}]-exendin-4 were first incubated with INS-1 cells in 24-well plates for 1 h at 37 °C. The cells were washed three times with chilled PBS and allowed to stand with fresh buffer at 37 °C. At various time points (0, 30 and 60 min), the medium was removed and the cells washed three times with chilled PBS. The cells were then lysed with 200 μL 0.1 M NaOH. The cell suspensions were collected and measured in a gamma counter. Each data point is an average of triplicate values.

MicroPET imaging

PET scans and image analysis were performed using an Inveon microPET scanner (Siemens Medical Solutions). [^{18}F]FPenM-[cys^{40}]-exendin-4 (~100 μCi) was administered *via* tail vein injection while the animal was under isoflurane anesthesia. Five-minute and ten-minute static PET images were acquired at 30 min and 60 min post-injection (p.i.; n = 4/group), respectively. For blocking experiment, 75 μg [cys^{40}]-exendin-4 was injected 10 min prior to the injection of [^{18}F]FPenM-[cys^{40}]-exendin-4. The images were reconstructed using a three-dimensional ordered-subset expectation maximization (3D OSEM) algorithm without correction for attenuation or scattering. For each scan, regions of interest (ROIs) were drawn over the tumor and major organs using Inveon Workplace 3.0 on decay-corrected whole-body coronal images. The radioactivity concentrations within the tumors, muscle, liver, and kidneys were obtained from mean pixel values within the multiple ROI volume and then

converted to MBq/mL/min using the calibration factor determined for the Inveon PET system. These values were then divided by the administered activity to obtain (assuming a tissue density of 1 g/mL) an image-ROI-derived percent injected dose per gram (%ID/g).

Biodistribution studies and metabolite analysis

Immediately after PET imaging, the tumor-bearing mice were sacrificed and dissected. Blood, tumor, major organs, and tissues were collected and wet-weighed. The radioactivity in the wet whole tissue was measured with a γ-counter (Wallach Wizard, PerkinElmer). The results were expressed as percentage of injected dose per gram of tissue (%ID/g) for a group of 4 animals. For each mouse, the radioactivity of the tissue samples was calibrated against a known aliquot of the injected radiotracer. Values were expressed as mean ± SD. For a blocking study, tumor xenografted mice were pretreated with 75 μg [cys^{40}]-exendin-4 10 min prior to injection of the corresponding [^{18}F]FPenM-[cys^{40}]-exendin-4. A subset of the collected tissues (homogenized tumor and kidneys, plasma, and urine) was extracted with a volume of CH_3CN equal to the weight of the sample. The mixtures were centrifuged and the supernatant separated from the pellet. Supernatants were analyzed by HPLC using on-line radioactivity detection or via collection of 1 min fractions and subsequent γ-counting.

Results

Synthesis

N-2-Fluoroethylmaleimide **2** was prepared from commercially available 2-fluoroethylamine hydrochloride with a straightforward strategy (Scheme 1). *N*-methoxycarbonylmaleimide **1**, was subjected to reaction with 2-fluoroethylamine hydrochloride in saturated sodium bicarbonate solution to give fluoroethylmaleimide standard **2** [41]. The condensation was performed at 0 °C, and worked up immediately upon completion as indicated by thin layer chromatography. Extended reaction time at room temperature resulted in hydrolytic decomposition of the maleimide.

The *N*-3-fluoropropylmaleimide and *N*-5-fluoropentylmaleimide were obtained from similar procedures (Scheme 1). Firstly commercially available 1,3-propanediol **3b** and 1,5-pentanediol **3c** were converted into the corresponding di-tosylate **4b** and **4c** respectively. S_N2 displacement of one tosylate of **4b** and **4c** with di-*tert*-butyl iminodicarboxylate afforded compounds **5b** and **5c**, respectively, according to the reported procedure[40]. With **5b** and **5c** in hand, fluorine incorporation was achieved by displacement of the remaining tosylate with K_{222}/KF. Deprotection of the Boc functional group with TFA at room temperature afforded the free fluoroalkylamine. The conjugation between resulting primary amine intermediate and *N*-methoxycarbonylmaleimide proceeded smoothly under aqueous conditions as described above. N-3-fluoropropylmaleimide **8b** and N-5-fluoropentylmaleimide **8c** were obtained in 28% and 62% yield, respectively in three steps after silica gel chromatography. Compounds **2** and **8b** are colorless solids while **8c** is light yellow liquid. The conjugation of **2** and **8c** with [cys^{40}]-exendin-4 proceeded smoothly in PBS buffer with 0.1% sodium ascorbate as the antioxidant.

The three synthesized compounds **5a, 5b**, and **5c** with different aliphatic chains (ethyl, propyl and pentyl, respectively) were evaluated for labeling with ^{18}F (Scheme 2). For substrate **5a**, the radiofluorination proceeded in low yield (20–30%, decay uncorrected), perhaps due to the volatility of the resulting product. However, when propyl analogue **5b** and pentyl analogue **5c** were employed as the substrates, the fluorine incorporation in the first step typically afforded 50% and 65% decay uncorrected yields, respectively. After deprotection of the amine with TFA, the resulting fluoroalkylamine salt was subjected to reaction with *N*-methoxycarbonylmaleimide. The optimized conditions for this exchange

reaction employed saturated $NaHCO_3$/THF (3/1, v/v) as solvent and 0 °C as the reaction temperature. A 10-fold excess of *N*-methoxycarbonylmaleimide **1** (60 μmol) relative to substrate **5b** or **5c** (6 μmol) was used to shorten the reaction time to 5 min. Poor trapping efficiency was observed for product [^{18}F]**8b**, but product [^{18}F]**8c** with its longer aliphatic chain was readily purified and isolated from HPLC eluate. The overall yield of the three-step production of [^{18}F]**8c** based on initial [^{18}F]fluoride was 11–17% (uncorrected) after purification and isolation by HPLC. The entire synthesis procedure was completed in an average time of 110 min with product specific activity of 20–49 GBq/μmol. [^{18}F]FPenM was chosen as the prosthetic group for coupling with [cys^{40}]-exendin-4 according to the typical procedure [34].

Receptor binding assay

IC_{50} values of exendin-4, FBEM-[cys^{40}]-exendin-4, FEtM-[cys^{40}]-exendin-4 and FPenM-[cys^{40}]-exendin-4 against ^{125}I-GLP-1 in INS-1 cells are shown in Figure 3. Of the two modified tracers synthesized, FPenM-[cys^{40}]-exendin-4 has comparable IC_{50} (1.11 nM) with parent exendin-4 (0.98 nM), which also showed almost the same binding affinity as FBEM-[cys^{40}]-exendin-4 (1.10 nM). FEtM-[cys^{40}]-exendin-4 exhibited slightly lower binding affinity (1.57 nM) compared to parent exendin-4 and FBEM-[cys^{40}]-exendin-4. These results indicated that labeling [cys^{40}]-exendin-4 with our newly developed FPenM did not reduce binding affinity towards INS-1 cells.

Mouse serum stability

Serum stability, as analyzed by radioHPLC, showed that [^{18}F]FPenM-[cys^{40}]-exendin-4 was stable in mouse serum up to 2.5 h at 37 °C, with only a negligible quantity of polar component produced (Figure S1), which may be due to the oxidation of the methionine in [cys^{40}]-exendin-4[34]. We found that the polar component could be minimized by adding $EDTANa_2$ to the analytical HPLC solvent as metal chelator during analysis. The extraction efficiency from the mouse serum was around 85% based on the supernatant fraction we injected for on-line radio-HPLC analysis.

Cell uptake and clearance

The total cell uptake kinetics of [^{18}F]FPenM-[cys^{40}]-exendin-4 with INS-1 tumors cells are shown in Figure 4. The cell uptake of [^{18}F]FPenM-[cys^{40}]-exendin-4 showed 0.62 ± 0.03 %AD at 0.5 h, increasing to 0.83 ± 0.06 %AD after 1 h, then the uptake reached a plateau. The cell efflux was performed after 60 min incubation, the cell retention was reduced to 0.89 ± 0.08 %AD at 30 min and 0.72 ± 0.06 %AD at 60 min. The specificity of the radiotracer was confirmed by minimum cell uptake of [^{18}F]FPenM-[cys^{40}]-exendin-4 (< 0.1%AD) in the presence of blocking dose of exendin-4 (1 μM).

Imaging and biodistribution in INS-1 xenograft

High tumor uptake was apparent by microPET imaging (Figure 5) at 30 min post-injection of [^{18}F]FPenM-[cys^{40}]-exendin-4 (21.30 ± 4.55 %ID/g), and remained virtually unchanged (20.32 ± 4.36% ID/g) at 60 min after tracer injection. In contrast, kidney uptake of [^{18}F]FPenM-[cys^{40}]-exendin-4 was high (34.41 ± 4.59 %ID/g) at 30 min and was significantly reduced by 60 min post-injection (11.30 ± 2.41 %ID/g). Similar clearance was observed from liver (3.36 ± 0.02 %ID/g at 30 min *vs.* 1.41 ± 0.02 %ID/g at 60 min). Negligible tracer uptake was observed in the muscle. Injection of a blocking dose of [cys^{40}]-exendin-4 prior to tracer injection resulted in significant reduction of tumor uptake at 30 min (2.65 ± 0.63 %ID/g), but kidney and liver uptake showed slight reduction, indicating receptor specific uptake of the tracer to INS-1 tumor. Quantification of the PET data at the 1 h time point showed high tumor-to-kidney (1.80) and tumor-to-liver (8.43) ratios. The

specific tumor uptake of [^{18}F]FPenM-[cys^{40}]-exendin-4 was further confirmed by biodistribution, which showed tumor-to-kidney and tumor-to-liver ratios of 1.75 and 28.14 respectively (Figure 6), and significant blocking was observed by injection of [cys^{40}]-exendin-4 prior to tracer administration. Negligible uptake was observed in the bone, indicating the stability of the tracer to defluorination. The blocking dose resulted in a reduction in uptake in the kidneys, pancreas, and lung.

The metabolic fate of the [^{18}F]FPenM-[cys^{40}]-exendin-4 in tumor, kidneys and urine were investigated by analysis of samples extracted following biodistribution studies in INS-1 tumor-bearing mice. The extracts from organs were analyzed by radio-HPLC and then compared to parent [^{18}F]FPenM-[cys^{40}]-exendin-4. The resulting radio-HPLC chromatograms indicated that urine contained only polar radioactive metabolites and the kidneys contained a mixture of parent [^{18}F]FPenM-[cys^{40}]-exendin-4 and polar radioactive metabolites; however, the tumor contained predominately parent peptide (Figure S2).

Discussion

We have developed a new thiol-specific prosthetic agent, [^{18}F]FPenM, based on aliphatic nucleophilic substitution No additional activating functional groups are required as in the case of homoaromatic fluorination. Because the maleimide ring is not stable under typical nucleophilic radiofluorination conditions, a three-step radiolabeling procedure was employed: 1) ^{18}F incorporation by S_N2 displacement on an aliphatic tosylate substrate; 2) TFA acidolysis of amine protecting group; 3) incorporation of [^{18}F]fluoroalkylamine into a maleimide via transamidation. Three tosylate substrates **5a, 5b**, and **5c**, with different lengths of aliphatic chains and hence different lipophilicity, were screened for ^{18}F labeling.

Substrate **5a** exhibited very low yield in the fluorination step, possibly due to the volatility of the resulting product. However, reaction of substrates **5b** and **5c** afforded higher yield for this labeling step. The subsequently produced fluoromaleimides **8a** and **8b** presented with an unanticipated problem.

Poor trapping efficiency was obtained for products [^{18}F]**8a** and [^{18}F]**8b** using solid-phase extraction of the crude reaction mixtures directly or from fractions following semi-preparative HPLC. However, product [^{18}F]**8c**, with its longer aliphatic chain, was much more efficiently isolated from the HPLC eluate. The high trapping efficiency for the most lipophilic [^{18}F]**8c** led us to apply this to the synthesis of [^{18}F]FPenM-[cys^{40}]-exendin-4.

We prepared authentic samples of FEtM-[cys^{40}]-exendin-4 and FPenM-[cys^{40}]-exendin-4 in order to evaluate the binding affinity relative to GLP-1. The binding affinities of exendin-4, FPenM-[cys^{40}]-exendin-4, and FBEM-[cys^{40}]-exendin-4 were about 1 nM and not significantly different from each other. These affinities are higher than previously reported NOTA-MAL-[cys^{40}]-exendin-4 (2.84 nM) [35] and [Lys^{40}(^{nat}Ga-DOTA)]exendin-3 (5.7 nM) [41]. [^{18}F]FPenM-[cys^{40}]-exendin-4 showed quite low uptake into INS-1 tumor cells. However, the efflux of radiolabeled compound was also quite slow. This cell uptake and efflux behavior was similar to that reported for FBEM-[cys^{40}]-exendin-4[34].

In INS-1 tumor xenograft model, microPET imaging of [^{18}F]FPenM-[cys^{40}]-exendin-4 showed high tumor uptake at early time point (30 min), and remained almost the same at 60 min after tracer injection. The high tumor uptake can be significantly blocked by injection of unlabeled [cys^{40}]-exendin-4 prior to radiolabeled tracer administration, which indicated highly specific targeting towards INS-1 tumor of the labeled peptide. Kidney uptake was higher (33 %ID/g) than tumor at 30 min, but had cleared by a factor of 3 (11 %ID/g) by 60 min. This kidney retention is similar to that of [^{18}F]FBEM-[cys^{40}]-exendin-4 and much

lower compared to [^{18}F]AlF-NOTA-[cys^{0}]-exendin-4 [35] and [Lys^{40}(^{68}Ga-DOTA)]-exendin-3 [42], which showed 63 %ID/g and 120 %ID/g respectively at 60 min post-injection. We reported that kidney uptake of [^{18}F]AlF-NOTA-MAL-[cys^{40}]-exendin-4[35] increased throughout the course of a 60-min experiment. Evaluation of kidney uptake in non-tumor bearing mice using another exendin-4 analogue [^{18}F]AlF-NOTA-[cys^{0}]-exendin-4, in which NOTA is attached at the N-terminus of the peptide, also showed high and sustained kidney uptake in 60 min. High kidney uptake has been reported for all radiometal chelate exendin analogues[43–46]. The tumor-to-kidney and tumor-to-liver ratios at later time point were further confirmed by *ex vivo* biodistribution study. INS-1 tumor uptake of ^{18}F-FBEM-exendin-4 is 30.27 ± 5.44% ID/g[34], while that of the probe used in this study is 33.21 ± 4.79% ID/g. There is no significant difference as to tumor uptake with these two tracers. There was negligible uptake in bone, indicating the stability of the tracer to defluorination. Tracer uptake in pancreas and lung were both high and can be blocked by injection of unlabeled [cys^{40}]-exendin-4. This is consistent with the results reported by our group[34], which is due to the fact that GLP-1 receptor is mainly expressed in the pancreatic islet cell, the intestine, lung, kidneys, breast and brainstem. These results suggest that [^{18}F]FPenM-[cys^{40}]-exendin-4 specifically binds to GLP-1R expressing organs[47].

We showed by radioHPLC that [^{18}F]FPenM-[cys^{40}]-exendin-4 was stable in mouse serum over 2.5 h. An *ex vivo* metabolite study, conducted by tissue extraction, showed that most radioactivity in tumor was intact parent compound, but the kidneys contained a great deal of polar metabolites and that the urine contained only polar metabolites. Thus the tumor has very little retention of radioactive metabolites whether they were produced or not.

GLP-1R is an important target, both for insulinoma and for imaging pancreatic beta cells, which also present GLP-1R. Beta cell transplantation currently is used for treatment of patients with type I diabetes. Since GLP-1 receptor agonists, such as exendin-4 analogs, can selectively bind to GLP-1R, they can be potentially used for detection of insulinoma and to monitor the survival of transplanted beta cells. However, immunological rejections limit the survival of the transplant. ^{18}F labeled exendin-4 could potentially be used to monitor the viability and mass of transplanted beta cells [41]. The utility of the exendin-4 analogs depends on achieving high signal to background ratio, especially in the abdomen where most insulinomas are found. In addition, beta cell transplantation is often conducted in the liver [48, 49]. Our results indicated specific uptake of [^{18}F]FPenM-[cys^{40}]-exendin-4 in tissues containing GLP-1R. Uptake is problematic in the kidneys, but the majority of gastrointestinal tract and liver had very low background radioactivity. Thus it may prove useful as a PET imaging agent for insulinoma and pancreas imaging.

Conclusion

A new prosthetic group, [^{18}F]FPenM, for site-specific labeling of free thiol group in proteins and peptides was developed. To the best of our knowledge, this is the first example of maleimide-containing prosthetic group synthesized based on aliphatic nucleophilic substitution and it has the smallest molecular weight among the developed prosthetic agents. Since the maleimido group was incompatible with harsh radiofluorination conditions, three synthetic steps were required for the prosthetic group synthesis. Thus, we achieved no improvement in yields or synthetic simplification compared to [^{18}F]FBEM.. The application of [^{18}F]FPenM was demonstrated in the synthesis and evaluation of [^{18}F]FPenM-[cys^{40}]-exendin-4 for imaging GLP-1R. The tracer has comparable imaging results with [^{18}F]FBEM-[cys^{40}]-exendin-4 developed by our group, showing high tumor-to-liver and tumor-to-kidney uptake ratios for GLP-1R imaging. INS-1 tumor xenografts, pancreas and lung showed specific uptake, indicating that [^{18}F]FPenM-[cys^{40}]-exendin-4 may be useful as pancreatic β-cell imaging agent. The developed tracer has higher binding affinity than

NOTA-MAL-[cys^{40}]-exendin-4 and [Lys^{40}(^{nat}Ga-DOTA)]exendin-3, superior tumor targeting and more rapid kidney clearance, showing it is a promising imaging probe for *in vivo* targeting of insulinomas.

Supplementary Material

Refer to Web version on PubMed Central for supplementary material.

Acknowledgments

This work was supported by the intramural research program of the National Institute of Biomedical Imaging and Bioengineering, National Institutes of Health. The authors acknowledge the NIH Warren Grant Magnuson Clinical Center's PET Department for radioisotope production. Lei Zhu was partially supported by the Center for Neuroscience and Regenerative Medicine (CNRM) through Henry Jackson Foundation

REFERENCES

1. Reubi JC. Peptide receptors as molecular targets for cancer diagnosis and therapy. Endocr Rev. 2003; 24:389–427. [PubMed: 12920149]
2. Sideris L, Dube P, Rinke A. Antitumor effects of somatostatin analogs in neuroendocrine tumors. Oncologist. 2012; 17:747–755. [PubMed: 22628056]
3. Wilbur DS. Radiohalogenation of proteins: an overview of radionuclides, labeling methods, and reagents for conjugate labeling. Bioconjugate Chem. 1992; 3:433–470.
4. Couturier O, Luxen A, Chatal JF, Vuillez JP, Rigo P, Hustinx R. Fluorinated tracers for imaging cancer with positron emission tomography. Eur J Nucl Med Mol Imaging. 2004; 31:1182–1206. [PubMed: 15241631]
5. Miller PW, Long NJ, Vilar R, Gee AD. Synthesis of ^{11}C, ^{18}F, ^{15}O, and ^{13}N radiolabels for positron emission tomography. Angew Chem Int Ed. 2008; 47:8998–9033.
6. Chen K, Conti PS. Target-specific delivery of peptide-based probes for PET imaging. Adv Drug Deliv Rev. 2010; 62:1005–1022. [PubMed: 20851156]
7. Ting R, Adam MJ, Ruth TJ, Perrin DM. Arylfluoroborates and alkylfluorosilicates as potential PET imaging agents: high-yielding aqueous biomolecular ^{18}F-labeling. J Am Chem Soc. 2005; 127:13094–13095. [PubMed: 16173707]
8. Schirrmacher R, Bradtmoller G, Schirrmacher E, Thews O, Tillmanns J, Siessmeier T, Buchholz HG, Bartenstein P, Wangler B, Niemeyer CM, Jurkschat K. ^{18}F-labeling of peptides by means of an organosilicon-based fluoride acceptor. Angew Chem Int Ed. 2006; 45:6047–6050.
9. Mu L, Hohne A, Schubiger PA, Ametamey SM, Graham K, Cyr JE, Dinkelborg L, Stellfeld T, Srinivasan A, Voigtmann U, Klar U. Silicon-based building blocks for one-step ^{18}F-radiolabeling of peptides for PET imaging. Angew Chem Int Ed. 2008; 47:4922–4925.
10. Becaud J, Mu L, Karramkam M, Schubiger PA, Ametamey SM, Graham K, Stellfeld T, Lehmann L, Borkowski S, Berndorff D, Dinkelborg L, Srinivasan A, Smits R, Koksch B. Direct one-step ^{18}F-labeling of peptides via nucleophilic aromatic substitution. Bioconjugate chem. 2009; 20:2254–2261.
11. Jacobson O, Zhu L, Ma Y, Weiss ID, Sun X, Niu G, Kiesewetter DO, Chen X. Rapid and simple one-step F-18 labeling of peptides. Bioconjugate chem. 2011; 22:422–428.
12. Mading P, Fuchtner F, Wust F. Module-assisted synthesis of the bifunctional labelling agent N-succinimidyl 4-[^{18}F]fluorobenzoate ([^{18}F]SFB). Appl Radiat Isot. 2005; 63:329–332. [PubMed: 15949940]
13. Vaidyanathan G, Zalutsky MR. Synthesis of N-succinimidyl 4-[^{18}F]fluorobenzoate, an agent for labeling proteins and peptides with ^{18}F. Nat Protoc. 2006; 1:1655–1661. [PubMed: 17487148]
14. Jacobson O, Chen X. PET designated flouride-18 production and chemistry. Curr Top Med Chem. 2010; 10:1048–1059. [PubMed: 20388116]
15. Kuchar M, Pretze M, Kniess T, Steinbach J, Pietzsch J, Loser R. Site-selective radiolabeling of peptides by ^{18}F-fluorobenzoylation with [^{18}F]SFB in solution and on solid phase: a comparative study. Amino Acids. 2012; 43:1431–1443. [PubMed: 22302364]

16. Jahan M, Nag S, Krasikova R, Weber U, Muhs A, Pfeifer A, Spenger C, Willbold D, Gulyas B, Halldin C. Fluorine-18 labeling of three novel D-peptides by conjugation with N-succinimidyl-4-[^{18}F]fluorobenzoate and preliminary examination by postmortem whole-hemisphere human brain autoradiography. Nucl Med Biol. 2012; 39:315–323. [PubMed: 22136889]
17. Jacobson O, Weiss ID, Kiesewetter DO, Farber JM, Chen X. PET of tumor CXCR4 expression with 4-^{18}F-T140. J Nucl Med. 2010; 51:1796–1804. [PubMed: 20956475]
18. Yang CY, Gu ZW, Yang M, Lin SN, Garcia-Prats AJ, Rogers LK, Welty SE, Smith CV. Selective modification of apoB-100 in the oxidation of low density lipoproteins by myeloperoxidase in vitro. J Lipid Res. 1999; 40:686–698. [PubMed: 10191293]
19. Fu X, Mueller DM, Heinecke JW. Generation of intramolecular and intermolecular sulfenamides, sulfinamides, and sulfonamides by hypochlorous acid: a potential pathway for oxidative cross-linking of low-density lipoprotein by myeloperoxidase. Biochemistry. 2002; 41:1293–1301. [PubMed: 11802729]
20. Beilan HS, Kenyon GL, Browne DT. Incorporation of specifically labeled cysteine into Escherichia coli protein. Anal Biochem. 1983; 128:169–174. [PubMed: 6342463]
21. Kolmar H. Alternative binding proteins: biological activity and therapeutic potential of cystine-knot miniproteins. FEBS J. 2008; 275:2684–2690. [PubMed: 18435757]
22. Shiue CY, Wolf AP, Hainfeld JF. Synthesis of ^{18}F-labelled N-(p-[^{18}F]fluorophenyl)maleimide and its derivatives for labelling monoclonal antibody with ^{18}F. J Labelled Compd Radiopharm. 1989; 26:287–289.
23. Toyokuni T, Walsh JC, Dominguez A, Phelps ME, Barrio JR, Gambhir SS, Satyamurthy N. Synthesis of a new heterobifunctional linker, N-[4-(aminooxy)butyl]maleimide, for facile access to a thiol-reactive ^{18}F-labeling agent. Bioconjugate chem. 2003; 14:1253–1259.
24. Berndt M, Pietzsch J, Wuest F. Labeling of low-density lipoproteins using the ^{18}F-labeled thiol-reactive reagent N-[6-(4-[^{18}F]fluorobenzylidene)aminooxyhexyl]maleimide. Nucl Med Biol. 2007; 34:5–15. [PubMed: 17210457]
25. Wuest F, Kohler L, Berndt M, Pietzsch J. Systematic comparison of two novel, thiol-reactive prosthetic groups for ^{18}F labeling of peptides and proteins with the acylation agent succinimidyl-4-[^{18}F]fluorobenzoate ([^{18}F]SFB). Amino Acids. 2009; 36:283–295. [PubMed: 18414978]
26. Wuest F, Berndt M, Bergmann R, van den Hoff J, Pietzsch J. Synthesis and application of [^{18}F]FDG-maleimidehexyloxime ([^{18}F]FDG-MHO): a [^{18}F]FDG-based prosthetic group for the chemoselective ^{18}F-labeling of peptides and proteins. Bioconjugate chem. 2008; 19:1202–1210.
27. de Bruin B, Kuhnast B, Hinnen F, Yaouancq L, Amessou M, Johannes L, Samson A, Boisgard R, Tavitian B, Dolle F. 1-[3-(2-[^{18}F]fluoropyridin-3-yloxy)propyl]pyrrole-2,5-dione: design, synthesis, and radiosynthesis of a new [^{18}F]fluoropyridine-based maleimide reagent for the labeling of peptides and proteins. Bioconjugate Chem. 2005; 16:406–420.
28. Cai W, Zhang X, Wu Y, Chen X. A thiol-reactive ^{18}F-labeling agent, N-[2-(4-^{18}F-fluorobenzamido)ethyl]maleimide, and synthesis of RGD peptide-based tracer for PET imaging of alpha v beta 3 integrin expression. J Nucl Med. 2006; 47:1172–1180. [PubMed: 16818952]
29. Wang H, Gao H, Guo N, Niu G, Ma Y, Kiesewetter DO, Chen X. Site-specific labeling of scVEGF with fluorine-18 for positron emission tomography imaging. Theranostics. 2012; 2:607–617. [PubMed: 22768028]
30. Koslowsky I, Mercer J, Wuest F. Synthesis and application of 4-[^{18}F]fluorobenzylamine: A versatile building block for the preparation of PET radiotracers. Org Biomol Chem. 2010; 8:4730–4735. [PubMed: 20740244]
31. Inkster JA, Liu K, Ait-Mohand S, Schaffer P, Guerin B, Ruth TJ, Storr T. Sulfonyl fluoride-based prosthetic compounds as potential ^{18}F labelling agents. Chem Eur J. 2012; 18:11079–11087. [PubMed: 22807282]
32. McBride WJ, D'Souza CA, Sharkey RM, Goldenberg DM. The radiolabeling of proteins by the [^{18}F]AlF method. Appl Radiat Isot. 2012; 70:200–204. [PubMed: 21890371]
33. Dolle F. Fluorine-18-labelled fluoropyridines: advances in radiopharmaceutical design. Curr Pharm Des. 2005; 11:3221–3235. [PubMed: 16250851]

34. Kiesewetter DO, Gao H, Ma Y, Niu G, Quan Q, Guo N, Chen X. ^{18}F-radiolabeled analogs of exendin-4 for PET imaging of GLP-1 in insulinoma. Eur J Nucl Med Mol Imaging. 2012; 39:463–473. [PubMed: 22170321]
35. Kiesewetter DO, Guo N, Guo J, Gao H, Zhu L, Ma Y, Niu G, Chen X. Evaluation of an [^{18}F]AlF-NOTA analog of exendin-4 for imaging of GLP-1 receptor in insulinoma. Theranostics. 2012; 2:999–1009. [PubMed: 23139727]
36. Keller O, Rudinger J. Preparation and some properties of maleimido acids and maleoyl derivatives of peptides. Helv Chim Acta. 1975; 58:531–541. [PubMed: 1158728]
37. Mohler DL, Shen G. The synthesis of tethered ligand dimers for PPARgamma-RXR protein heterodimers. Org Biomol Chem. 2006; 4:2082–2087. [PubMed: 16729120]
38. Bell TW, Choi HJ, Harte W, Drew MG. Syntheses, conformations, and basicities of bicyclic triamines. J Am Chem Soc. 2003; 125:12196–12210. [PubMed: 14519005]
39. Walczak RM, Cowart JS, Reynolds JR. Tethered PProDOTs: conformationally restricted 3,4-propylenedioxythiophene based electroactive polymers. J Mater Chem. 2007; 17:254–260.
40. Kiesewetter DO, Sassaman MB, Robbins J, Jagoda EM, Carson RE, Appel NM, Sutkowski E, Herscovitch P, Braun A, Eckelman WC. Synthesis and evaluation of an F-18 analog of forskolin for imaging adenylyl cyclase. J Fluorine Chem. 2000; 101:297–304.
41. Zhang Y, Chen W. Radiolabeled glucagon-like peptide-1 analogues: a new pancreatic beta-cell imaging agent. Nucl Med Commun. 2012; 33:223–227. [PubMed: 22262216]
42. Brom M, Oyen WJ, Joosten L, Gotthardt M, Boerman OC. ^{68}Galabelled exendin-3, a new agent for the detection of insulinomas with PET. Eur J Nucl Med Mol Imaging. 2010; 37:1345–1355. [PubMed: 20111963]
43. Wild D, Wicki A, Mansi R, Behe M, Keil B, Bernhardt P, Christofori G, Ell PJ, Macke HR. Exendin-4-based radiopharmaceuticals for glucagonlike peptide-1 receptor PET/CT and SPECT/CT. J Nucl Med. 2010; 51:1059–1067. [PubMed: 20595511]
44. Wild D, Behe M, Wicki A, Storch D, Waser B, Gotthardt M, Keil B, Christofori G, Reubi JC, Macke HR. [Lys^{40}(Ahx-DTPA-^{111}In)NH_2]exendin-4, a very promising ligand for glucagon-like peptide-1 (GLP-1) receptor targeting. J Nucl Med. 2006; 47:2025–2033. [PubMed: 17138746]
45. Wicki A, Wild D, Storch D, Seemayer C, Gotthardt M, Behe M, Kneifel S, Mihatsch MJ, Reubi JC, Macke HR, Christofori G. [Lys^{40}(Ahx-DTPA-^{111}In)NH_2]-Exendin-4 is a highly efficient radiotherapeutic for glucagon-like peptide-1 receptor-targeted therapy for insulinoma. Clin Cancer Res. 2007; 13:3696–3705. [PubMed: 17575235]
46. Brom M, Joosten L, Oyen WJ, Gotthardt M, Boerman OC. Radiolabelled GLP-1 analogues for in vivo targeting of insulinomas. Contrast Media Mol Imaging. 2012; 7:160–166. [PubMed: 22434628]
47. Baggio LL, Drucker DJ. Biology of incretins: GLP-1 and GIP. Gastroenterology. 2007; 132:2131–2157. [PubMed: 17498508]
48. Sahu S, Tosh D, Hardikar AA. New sources of beta-cells for treating diabetes. J Endocrinol. 2009; 202:13–16. [PubMed: 19420008]
49. Robertson RP. Islet transplantation as a treatment for diabetes - a work in progress. N Engl J Med. 2004; 350:694–705. [PubMed: 14960745]

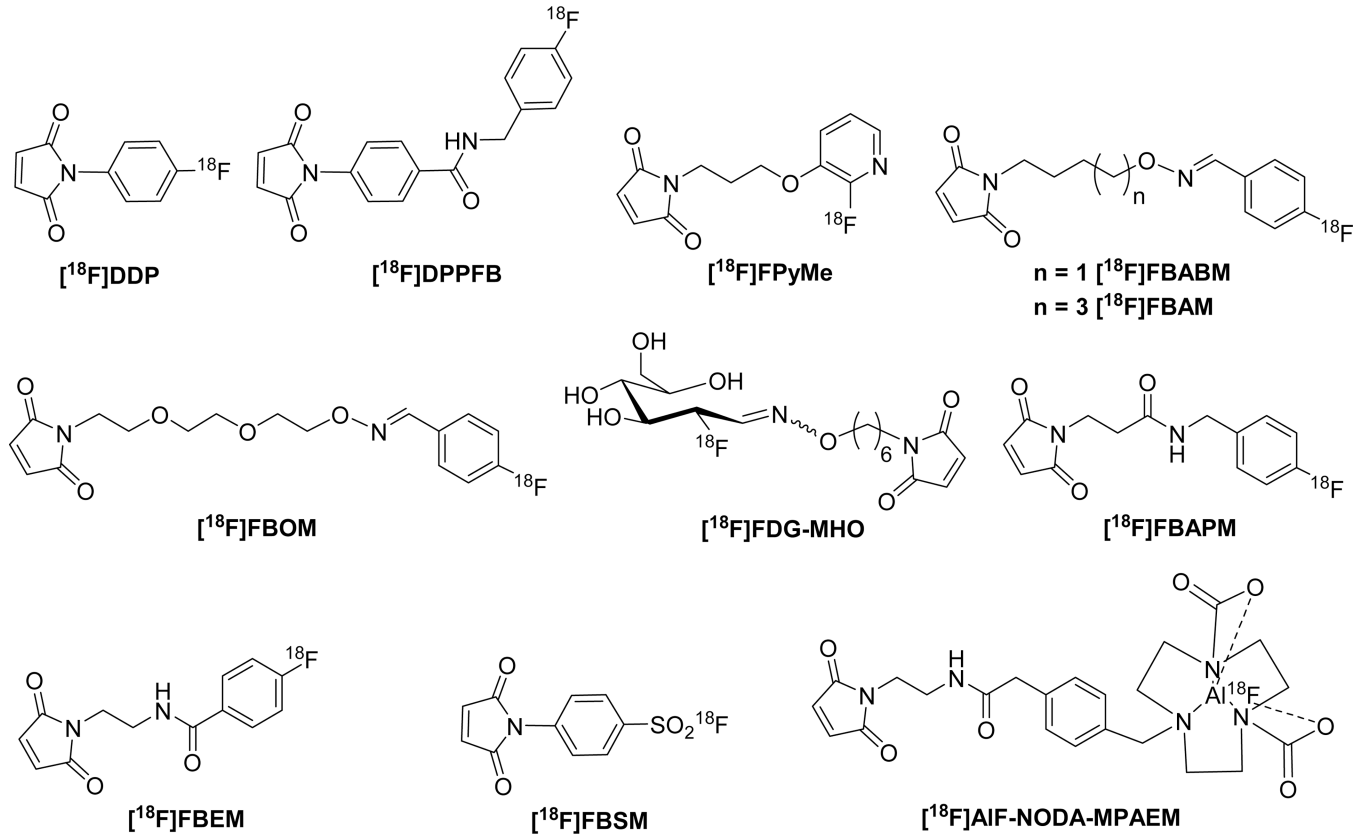

Figure 1.
^{18}F-labeled thiol site-specific prosthetic groups.

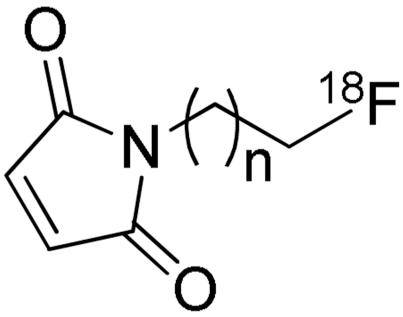

n = 1, *N*-2-[^{18}F]fluoroethylmaleimide (**[^{18}F]FEtM**)

n = 2, *N*-3-[^{18}F]fluoropropylmaleimide (**[^{18}F]FProM**)

n = 4, *N*-5-[^{18}F]fluoropentylmaleimide (**[^{18}F]FPenM**)

Figure 2.
N-[^{18}F]fluoroalkylmaleimide prosthetic groups.

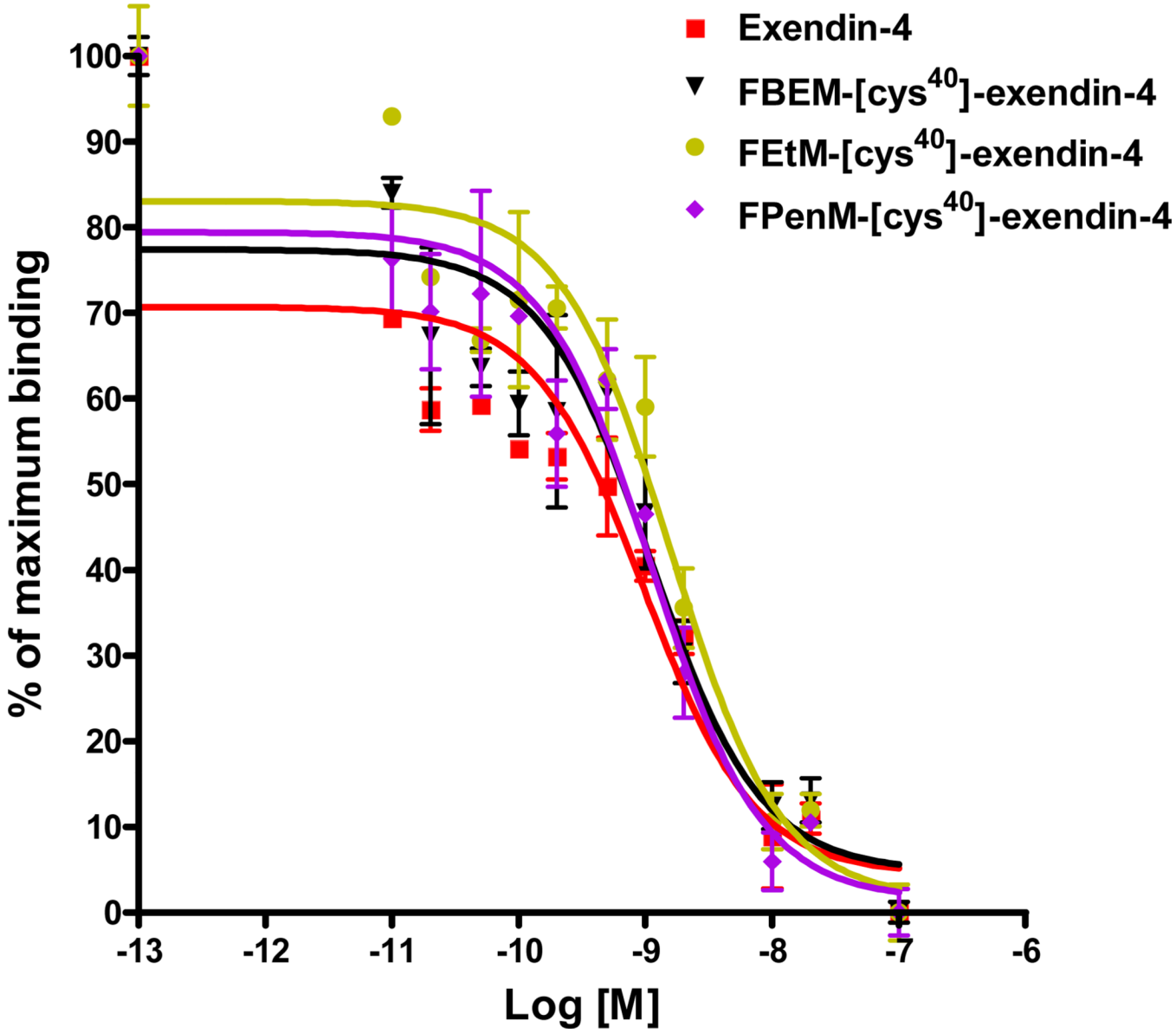

Figure 3.

Competitive binding assay (IC_{50}) of exendin-4 (■, red), FBEM-[cys^{40}]-exendin-4 (▼, black), FEtM-[cys^{40}]-exendin-4 (●, brown yellow), and FPenM-[cys^{40}]-exendin-4 (♦, purple).

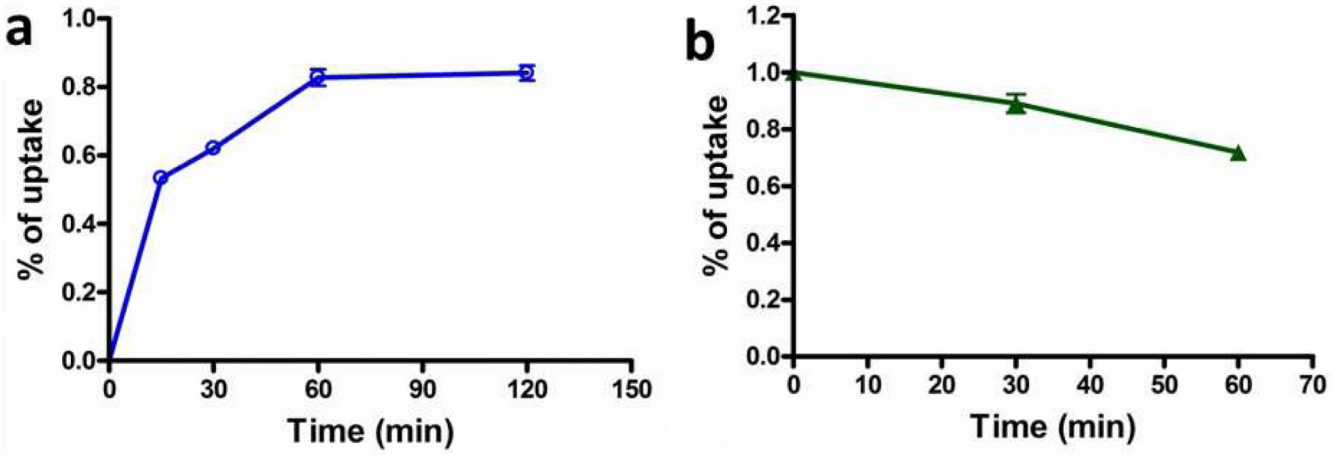

Figure 4.
Total cellular uptake (a, ○, blue) and efflux (b, ▲, green) of [^{18}F]FPenM-[cys^{40}]-exendin-4.

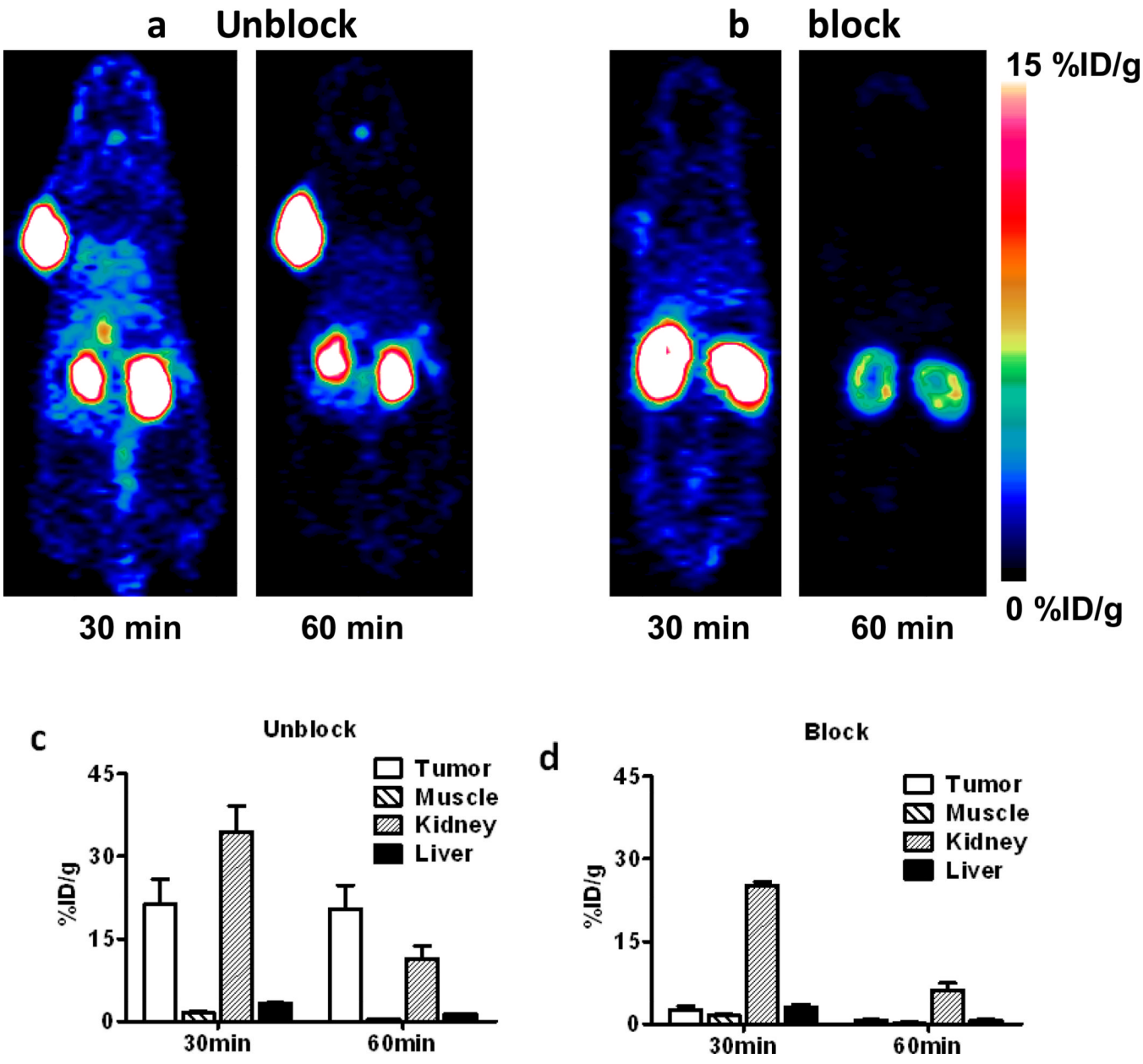

Figure 5.

Representative PET images of [^{18}F]FPenM-[cys^{40}]-exendin-4 (100 μCi) in INS-1 mouse xenograft models at 30 and 60 min post injection: (a) control; (b) INS-1 with a blocking dose of 75 μg [cys^{40}]-exendin-4 administered 10 min prior to the radiotracer; (c) time course of uptake by selected tissues determined by quantification of PET ROIs; (d) time course of uptake by selected tissues determined by quantification of PET ROIs following blocking dose.

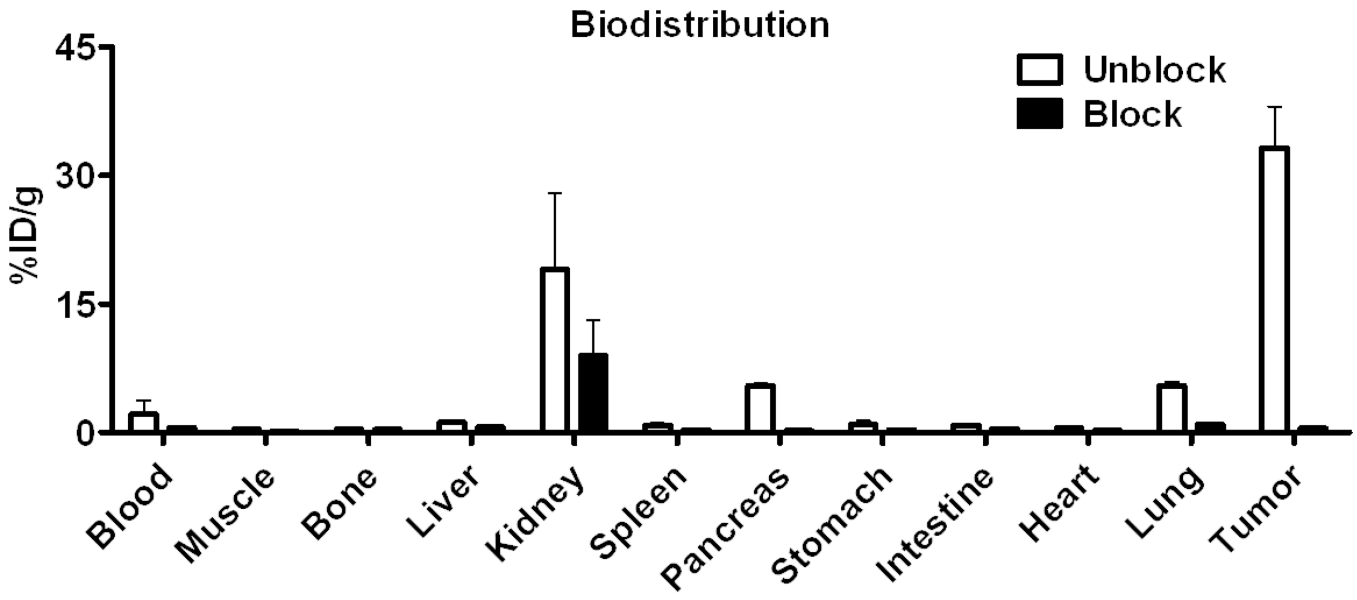

Figure 6.

Biodistribution of [^{18}F]FPenM-[cys^{40}]-exendin-4 (100 μCi) at 1 h measured by radioactive counting of dissected tissues with or without [cys^{40}]-exendin-4 (75 μg) blocking dose prior to tracer injection.

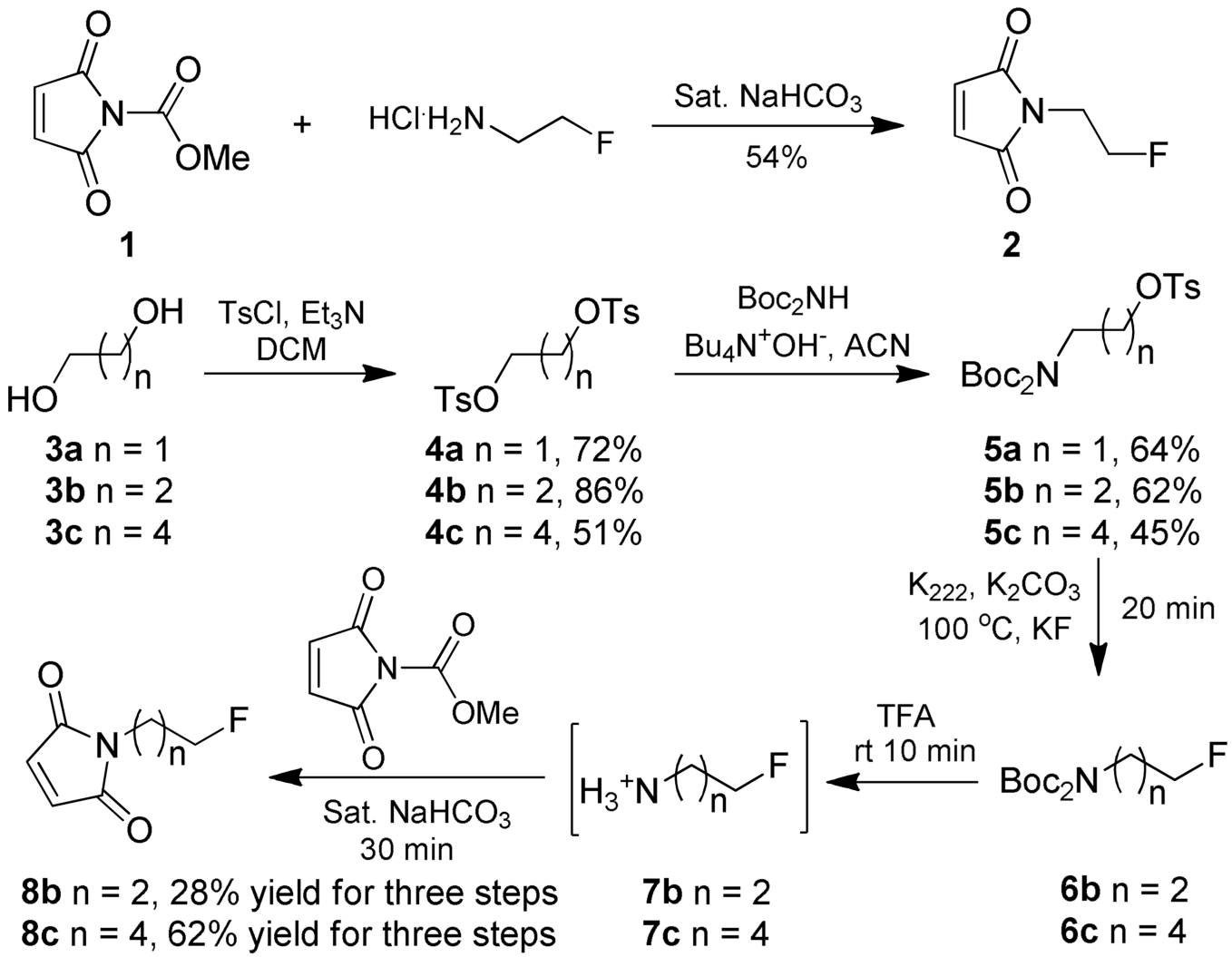

Scheme 1.

Synthesis of *N*-2-fluoroethylmaleimide **2***N*-3-fluoropropylmaleimide **8b***N-5*-fluoropentylmaleimide standards **8c** respectively.

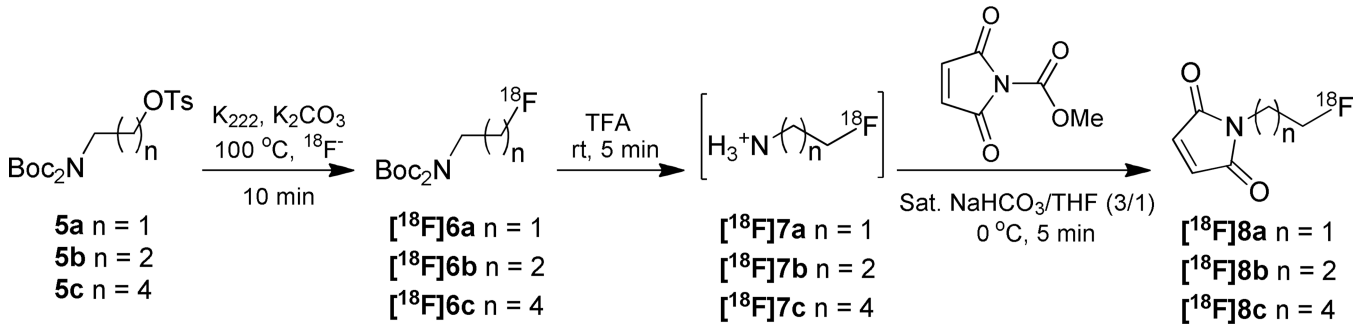

Scheme 2.
^{18}F radiolabeling of tosylate substrates **5a, 5b, 5c**.